WAVELET TRANSFORM IN SIGNAL AND IMAGE RESTORATION

A. Procházka*, J. Ptáček*, and I. Šindelářová†

* Prague Institute of Chemical Technology, Department of Computing and Control Engineering
Technická 1905, 166 28 Prague 6, Czech Republic
Phone: (+420) 224 354 198 * Fax: (+420) 224 355 053 * E-mail: {A.Prochazka, J.Ptacek}@ieee.org

† University of Economics, Department of Econometrics
W. Churchill Sq. 4, 130 67 Prague 3, Czech Republic
Phone: (+420) 224 095 443 * Fax: (+420) 224 095 423 * E-mail: ISin@vse.cz

Keywords: Discrete wavelet transform, wavelet decomposition and reconstruction, biomedical image analysis, image regions recovery, image enhancement, computer intelligence

Abstract

The paper presents selected mathematical methods of digital signal and image processing based upon the use of wavelet transform and signal decomposition with applications in system identification, analysis and modelling. The main part of the paper is devoted to signal de-noising using hard and soft thresholding and to the recovery of degraded parts of signals and images. The wavelet transform approach has been adopted here and used for the recovery of the corrupted image regions as an alternative to probabilistic models. Proposed methods present results of the iterated wavelet transform interpolation of missing signal and image components both for simulated signals and biomedical magnetic resonance images. Resulting algorithms are closely related to signal segmentation, change points detection and prediction with the use in process control, computer vision, signal or image processing and computer intelligence.

1 Introduction

A fundamental problem encountered in the interdisciplinary area of digital signal and image processing [7, 10, 11, 19] is in the selection of methods for signal and image analysis, segmentation, de-noising [8, 17, 19], recovery of its missing or corrupted components [1, 4, 6, 15, 20] and its enhancement [5, 12, 13, 14].

The paper presents selected methods and algorithms related to signal and image decomposition and reconstruction using wavelet transform [2, 3, 9, 16, 18] at first. Methods of wavelet decomposition are then used for signal de-noising and recovery of their corrupted parts using selected threshold limits. These methods were developed and verified for simulated one-dimensional and two-dimensional signals with additive noise components and then applied to processing of real biomedical images of human brain obtained by the magnetic resonance method.

All resulting algorithms are verified in the computational and visualization Matlab environment providing tools for remote signal processing using Matlab web server and computer network as well.

2 Principles of Discrete Wavelet Transform

Signal wavelet decomposition by wavelet transform (WT) provides an alternative to the discrete Fourier transform (DFT) for signal analysis allowing decomposition into two-dimensional functions of time and scale. The main benefit of WT over DFT is in its multi-resolution time-scale analysis ability.

Wavelet functions used for signal analysis are derived from the initial function $W(t)$ forming basis for the set of functions

$$W_{m,k}(t) = \frac{1}{\sqrt{a}}\, W\left(\frac{1}{a}\,(t-b)\right) = \frac{1}{\sqrt{2^m}}\, W\left(2^{-m}t - k\right) \qquad (1)$$

for discrete parameters of dilation $a = 2^m$ and translation $b = k\ 2^m$. Wavelet dilation, which is closely related to spectrum compression, enables local and global signal analysis.

3 Wavelet Decomposition and Reconstruction

The basic principle of signal and image wavelet decomposition and reconstruction is presented in Fig. 1. The same approach can be applied both to an image matrix $[g(n,m)]_{N,M}$ and to any one-dimensional signal considered as a special case of an image having one column only.

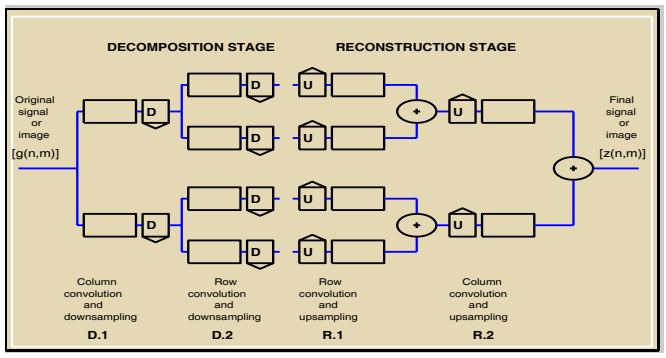

Figure 1: The principle of signal and image decomposition and reconstruction by wavelet transform

The decomposition stage includes the processing of the image matrix by columns at first using wavelet (high-pass) and scaling (low-pass) function. Let us denote a selected column of the image matrix $[g(n,m)]_{N,M}$ as signal $\{x(n)\}_{n=0}^{N-1} = [x(0), x(1), ..., x(N-1)]'$. This signal can be analyzed by a half-band low-pass filter with its impulse response

$$\{l(n)\}_{n=0}^{L-1} = [l(0), l(1), \cdots, l(L-1)] \tag{2}$$

and corresponding high-pass filter based upon impulse response

$$\{h(n)\}_{n=0}^{L-1} = [h(0), h(1), \cdots, h(L-1)] \tag{3}$$

The first stage of signal decomposition assumes the convolution of a given signal and the appropriate filter coefficients for decomposition by relations

$$x_l(n) = \sum_{k=0}^{L-1} l(k)\, x(n-k) \tag{4}$$

$$x_h(n) = \sum_{k=0}^{L-1} h(k)\, x(n-k) \tag{5}$$

for all values of n followed by subsampling by factor D. In the following step of signal decomposition the same process is applied to rows of the image matrix followed by row downsampling. The decomposition stage results in this way in four images representing all combinations of low-pass and high-pass initial image matrix processing.

The reconstruction stage includes row upsampling by factor U at first and row convolution at first. The corresponding images are then summed. The final step of image reconstruction assumes column upsampling and convolution with reconstruction filters followed by summation of the results again.

In the case of one-dimensional signal processing, steps $D.2$ and $R.1$ are omitted and the convolution mentioned above is applied to a column vector only. The whole process can be used for

1. Signal/image decomposition and perfect reconstruction using D=2 and U=2
2. Signal/image resolution enhancement in the case of D=1 and U=2
3. Signal/image de-noising based upon modification of image decomposition coefficients

4 Signal and Image De-noising

Wavelet transform coefficients both in the case of one-dimensional and two-dimensional signals can be organized in the column vector **c** combining all values evaluated in the decomposition stage up to the selected level. Undesirable signal components can be then eliminated applying appropriate threshold limits [18] to wavelet transform coefficients.

In the case of soft-thresholding it is possible to evaluate new coefficients $\overline{c}(k)$ using original coefficients $c(k)$ for a chosen limit δ by relation

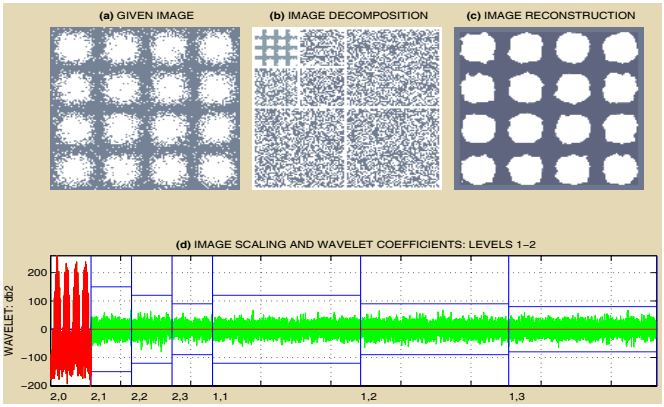

Figure 2: Simulated image de-noising presenting **(a)** given image, **(b)** image decomposition into two levels, **(c)** image reconstruction and **(d)** wavelet coefficients thresholding

$$\overline{c}(k) = \begin{cases} \text{sign } c(k)\ (|\,c(k)\,| - \delta) & \text{if } |\,c(k)\,| > \delta \\ 0 & \text{if } |\,c(k)\,| \leq \delta \end{cases} \tag{6}$$

Results of this process applied to a simulated signal are presented in Fig. 2 showing image decomposition into two levels resulting in wavelet coefficients both in the matrix form in Fig. 2(b) and in vector form according to Fig. 2(d). The level dependent thresholding is then applied to the vector of wavelet coefficients to obtain the final image in Fig. 2(c). Similar process has been further used for processing of real data representing a region of a biomedical magnetic resonance image with results given in Fig. 3 .

Table 1 presents results of a simulated image de-noising using selected wavelet functions, which give quite different wavelet coefficients because of their different definitions (analytic or numerical). Clearly, the wavelet transform provides then many ways for the wavelet decomposition of a given signal. The best result of given simulated image de-noising has been obtained by the Symmlet wavelet function of the 4th order. The second best result provides the Symmlet wavelet function of the 8th or-

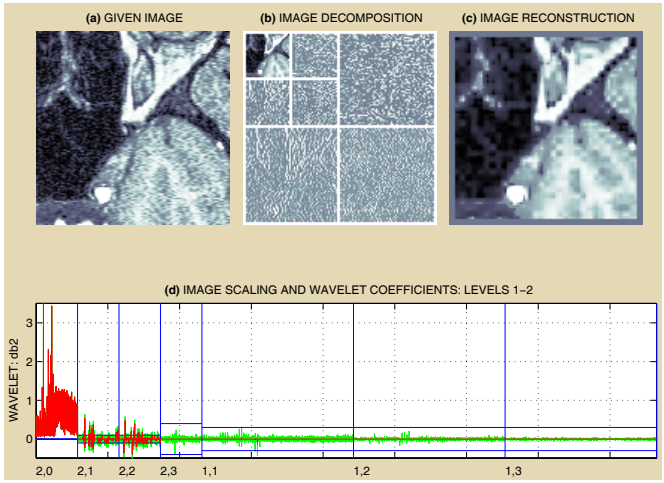

Figure 3: Real magnetic resonance image de-noising presenting **(a)** given image, **(b)** image decomposition into two levels, **(c)** image reconstruction and **(d)** coefficients thresholding

	De-noising - wavelet function	PSNR1 [dB]	PSNR2 [dB]
1	*Haar Wavelet*	13.266	21.000
2	*Wavelet Daubechies2*		20.838
3	*Wavelet Daubechies4*		24.528
4	*Wavelet Daubechies8*		24.315
5	*Wavelet Symmlet2*		20.838
6	*Wavelet Symmlet4*		24.873
7	*Wavelet Symmlet8*		24.713

Table 1: The peak-signal-to-noise-ratio (PSNR) of the simulated image with noise ($PSNR1$) and the same simulated image after de-noising ($PSNR2$) from the previous figure denoised by the selected wavelet functions

der. Criteria of an image de-noising quality include evaluation of peak-signal-to-noise-ratio (PSNR) value in dB.

Signal and image de-noising techniques are very important in the digital signal processing. They have wide ranging applications in the analysis of time series and image processing, particularly in image compression, transmission and reconstruction. Special attention is paid to biomedical images, the classification of their structures and detection of their specific components. Both two-dimensional discrete Fourier and wavelet transforms provide efficient methods to solve these problems in the frequency and time domains.

5 Signal and Image Regions Recovery

There are several types of signal information structures that can be used for their modelling and recovery of their missing or corrupted regions including

1. the correlation of each sample with the immediate neighbouring samples allowing autoregressive modelling or wavelet transform application
2. the correlation of each sample with samples from similar parts of signals useful particularly in signals with periodic texture patterns occurring at least in their separate regions
3. the probability distribution of signal segments

To obtain the best results these three types of structures and models can be combined to take advantage of all of the predictable information structure of the signal.

The presented method has been developed and checked out for periodical one-dimensional and two-dimensional signal and such signals with an additive noise.

Fig. 4 presents an example of the first step of corrupted signal region recovery. Simulated signal in Fig. 4(a) is decomposed providing its wavelet transform coefficients presented in its scalogram Fig. 4(c) and vector **c** with its values in Fig. 4(d). The first step of signal recovery assumes its thresholding and reconstruction resulting in values presented in Fig. 4(b).

The whole algorithm assumes that the wavelet coefficients in vector **c** are modified using hard thresholding by relation

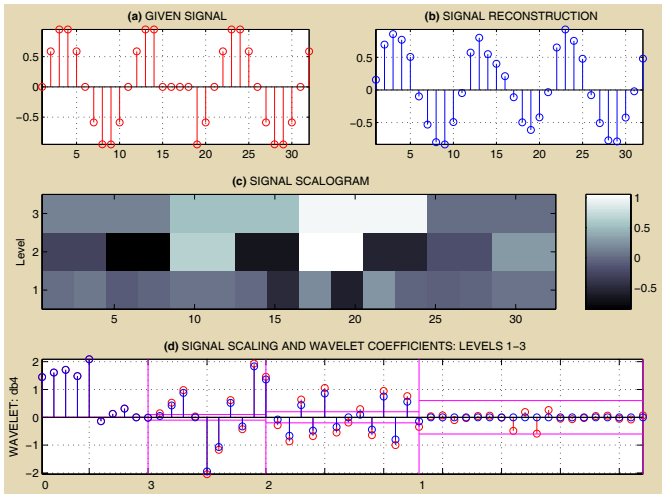

Figure 4: The first iteration of the reconstruction process of a one-dimensional signal presenting **(a)** given signal, **(b)** reconstructed signal after the first iteration, **(c)** signal decomposition into two levels, and **(d)** wavelet coefficients thresholding

$$\overline{c}(k) = \begin{cases} \mathrm{c}(k) & \text{if } |c(k)| > \delta \\ 0 & \text{if } |c(k)| \leq \delta \end{cases} \tag{7}$$

where δ is a threshold limit related the variance σ_e of coefficients noise e, and $\overline{c}(k)$ are thresholded coefficients. In the case that $\delta \sim \sigma_e$, then with a high probability $|\hat{c}| << |e|$, i.e., hard thresholding of vector **c** removes more noise than signal. This process preserves transform coefficients of high peak-signal-to-noise-ratio while zeroing out coefficients having lower PSNR.

The complete iterative algorithm changes just coefficients of the lost region of samples using hard thresholding to zero while all other values are preserved in each step. The algorithm is repeated until the sum of squared errors (SSE) between the recovered and the original signal is acceptably low or required PSNR [dB] is achieved. Fig. 5 presents results of such a process after 20 iterations.

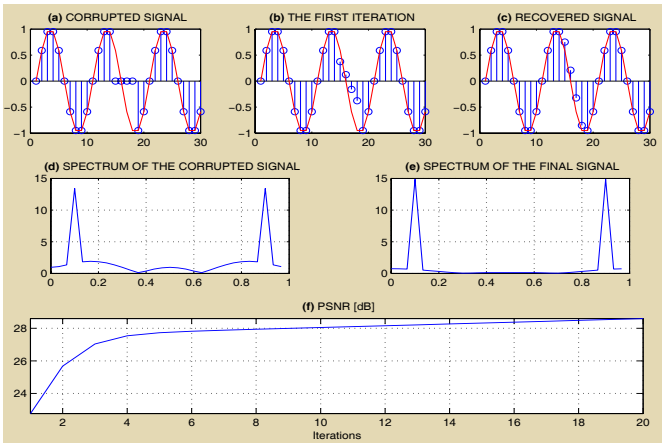

Figure 5: Simulated signal recovery process presenting **(a)** corrupted signal, recovered signal after **(b)** the first and **(c)** the final iteration of the recovery algorithm, spectrum estimation of the **(d)** initial and **(e)** the final signal (after 20 iterations), and **(f)** the peak-signal-to-noise-ratio evolution

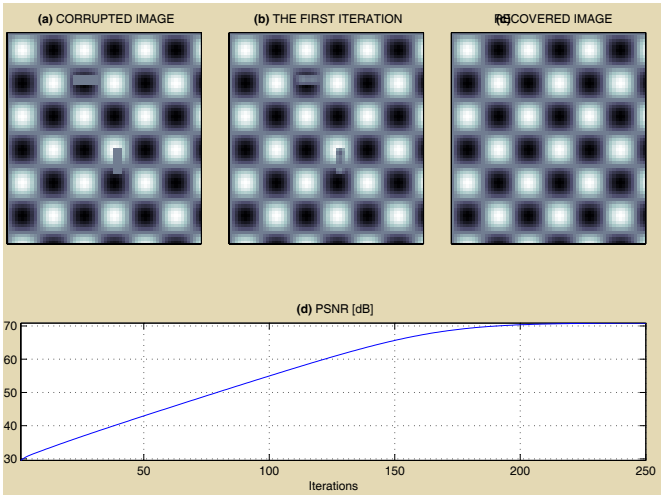

Figure 6: Simulated image recovery process presenting **(a)** corrupted image, recovered image after **(b)** the first and **(c)** the final iteration of the reconstruction algorithm, **(d)** the peak-image-to-noise-ratio evolution

The same technique has been applied to two-dimensional signals represented by a simulated image. The only difference is that the wavelet decomposition is implemented to rows at first followed by the same algorithm applied to columns according to Fig. 1. Result after the image wavelet decomposition, hard thresholding and wavelet backward reconstruction is presented in the Fig. 6 together with the evolution of the peak-signal-to-noise-ratio during the iteration process based upon the use of Daubechies wavelet function of the 4th order for image decomposition and reconstruction.

Table 2 provides results of the study of different wavelet functions use for reconstruction of image regions. Daubechies wavelet function of the 8th order provided the lowest SSE and the highest PSNR in this case.

Simulated perfect predictable signal presented in Fig. 6 was recovered at first. Two-dimensional sinwave function simulates an image without any additive noise component in this case. After 250 iterations a very good image recovery has been achieved with SSE almost equal to zero.

	Recovery - wavelet function	**PSNR1 [dB]**	**PSNR2 [dB]**	**SSE1**	**SSE2**
1	*Haar Wavelet*	28.849	30.969	21.356	13.107
2	*Daubechies2*		26.520		0.418
3	*Daubechies4*		70.872		0.001
4	*Daubechies8*		107.906		0.000
5	*Symmlet2*		26.520		0.418
6	*Symmlet4*		34.928		5.2682
7	*Symmlet8*		47.318		0.304

Table 2: The peak-signal-to-noise-ratio (PSNR) and sum of squared errors (SSE) of the simulated image containing corrupted regions ($PSNR1$, $SSE1$) and the same simulated image after the recovery algorithm ($PSNR2$, $SSE2$) reconstructed by the selected wavelet functions after 400 iterations

Another simulated image used for verification of the proposed algorithm is presented on Fig. 7. A very good result has been achieved after 100 iterations already. Original image has been decomposed by the Daubechies wavelet function of the 4th order again. The plot of the evolution of PSNR with respect to iteration steps is presented in Fig. 7 as well.

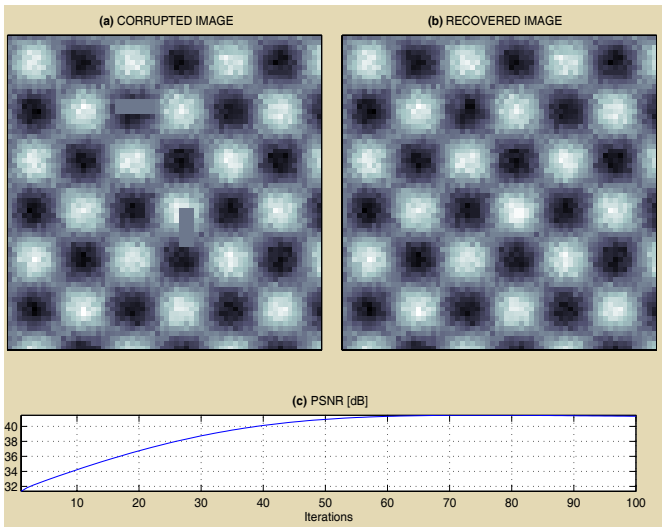

Figure 7: Recovery of a simulated image with an additional noise component presenting **(a)** given corrupted image and **(b)** recovered image (after 100 iterations), and **(c)** the peak-image-to-noise-ratio evolution

6 Results

Resulting iteration method of wavelet image regions recovery has been verified for simulated images at first and then applied to real magnetic resonance images of the brain. Selected result of the recovery of degraded part of this image is presented in Fig. 8. Efficiency of the recovery process provides good enough results even though they depend upon the degree and extension of corrupted image region and the choice of wavelet function.

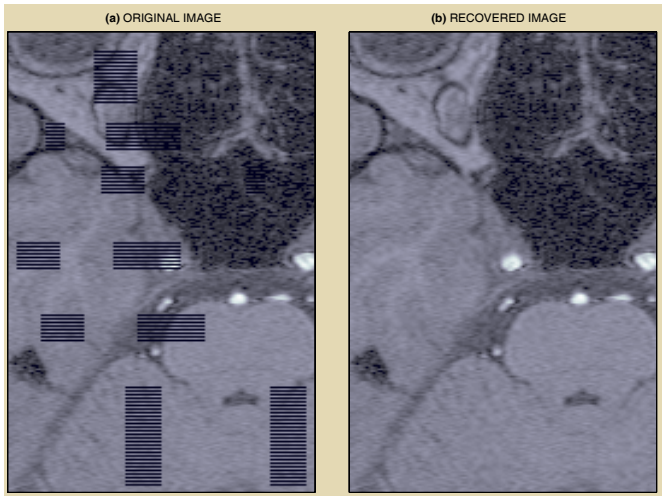

Figure 8: Recovery of a real biomedical image of the brain presenting **(a)** given corrupted image and **(b)** recovered image

7 Conclusion

There are many possibilities in the choice of appropriate transforms for signal decomposition including discrete Fourier transform, discrete cosine transform or discrete wavelet transform. The paper presents selected properties of the wavelet transform to achieve this goal using its ability to distinguish more frequency bands and to use different resolution at selected decomposition levels. The selection of different threshold limits for each decomposition level is presented in the paper as well. It is shown that the appropriate global or local threshold selection can be used both for signal or image de-noising and recovery of its corrupted regions using the iterative algorithm discussed in the paper.

Further study will be devoted to the appropriate estimation of threshold limits and to the the choice of wavelet functions. A special attention will be also paid to image enhancement by gradient methods and by the principal components analysis.

Selected results and algorithms can be obtained from the web page of the Prague DSP research group (http://dsp.vscht.cz) providing also access to the Matlab web server allowing remote data analysis and processing.

Acknowledgments

The work has been supported by the research grant of the Faculty of Chemical Engineering of the Institute of Chemical Technology, Prague No. MSM 223400007. All real MR images were kindly provided by the Faculty Hospital Královské Vinohrady in Prague.

References

[1] S. Armstrong, A.C. Kokaram, and P. Rayner. Reconstructing missing regions in colour images using multichannel median models. In *IXth European Signal Processing Conference EUSIPCO-98*, pages 1029–1032. European Association for Signal Processing, 1998.

[2] A. Bruce, D. Donoho, and Hong-Ye Gao. Wavelet Analysis. *IEEE Spectrum*, 33(10):26–35, October 1996.

[3] L. Debnath. *Wavelets and Signal Processing*. Birkhauser Boston, Boston, U.S.A., 2003.

[4] Alessandro Duci, Anthony J. Yezzi, Sanjoy K. Mitter, and Stefano Soatto. Region matching with missing parts. In *ECCV (3)*, pages 48–64, 2002.

[5] W. Etter. Restoration of Discrete-Time Signal Segments by Interpolation Based on the Left-Sided and Right-Sided Autoregressive Parameters. *IEEE Transaction on Signal Processing*, 44(5):1124–1135, May 1996.

[6] Onur G. Guleryuz. Iterated Denoising for Image Recovery. In *Data Compression Conference (DCC '02), Snao Bird, Utah*. IEEE, 2002.

[7] A. D. Kulkarni. *Computer Vision and Fuzzy-Neural Systems*. Prentice Hall PTR, Upper Saddle River, 2001.

[8] D. E. Newland. *An Introduction to Random Vibrations, Spectral and Wavelet Analysis*. Longman Scientific & Technical, Essex, U.K., third edition, 1994.

[9] N.G. Kingsbury and J.F.A. Mugarey. Wavelet Transforms in Image Processing. In A. Procházka, J. Uhlíř, P. J. W. Rayner, and N. G. Kingsbury, editors, *Signal Analysis and Prediction*, Applied and Numerical Harmonic Analysis, chapter 2. Birkhauser, Boston, U.S.A., 1998.

[10] M. Petrou and P. Bosdogianni. *Image Processing, The Fundamentals*. John Wiley & Sons, New York, 1999.

[11] I. Pitas. *Digital Image Processing Algorithms and Applications*. John Wiley & Sons, Inc., New York, 2000.

[12] A. Procházka, I. Šindelářová, and J. Ptáček. Image Denoising and Restoration Using Wavelet Transform. In *European Control Conference, Cambridge*. IEE London, 2003.

[13] J. Ptáček and A. Procházka. Autoregressive Modelling in Rejection of Image Artefacts. In *13th International Conference on Process Control, Štrbské Pleso, SK*. The Slovak Society of Cybernetics and Informatics, 2001.

[14] J. Ptáček, I. Šindelářová, A. Procházka, and J. Smith. Wavelet Transforms In Signal And Image Resolution Enhancement. In *16th International Conference Algoritmy 2002, Podbanske*. The Slovak Technical University, 2002.

[15] S. D. Rane, G. Sapiro, and M. Bertalmio. Structure and Texture Filling-In of Missing Image Blocks in Wireless Transmission and Compression Applications. *IEEE Trans. on Image Processing*, 12(3):296–303, 2003.

[16] O. Rioul and M. Vetterli. Wavelets and Signal Processing. *IEEE SP Magazine*, pages 14–38, October 1991.

[17] G. Strang. Wavelets and Dilation Equations: A brief introduction. *SIAM Review*, 31(4):614–627, Dec. 1989.

[18] G. Strang and T. Nguyen. *Wavelets and Filter Banks*. Wellesley-Cambridge Press, 1996.

[19] Saeed V. Vaseghi. *Advanced Digital Signal Processing and Noise Reduction*. Wiley & Teubner, West Sussex, U.K., second edition, 2000.

[20] Z. Wang, Y. Yu, and D. Zhang. Best Neighborhood Matching: An Information Loss Restoration Technique for Block-Based Image Coding Systems. *IEEE Transactions on Image Processing*, 7(7):1056–1061, July 1998.